

PREDICTIVE MODELLING OF MULTI-PERIOD GEOARCHAEOLOGICAL RESOURCES AT A RIVER CONFLUENCE

Phase 1 Report (PNUM 3357)

A. G. Brown¹, C. Carey¹, K. Challis², A. Howard³ & L. Cooper⁴

¹ School of Geography, Archaeology & Earth Resources, Amory Building, Rennes Drive, University of Exeter EX4 4RJ

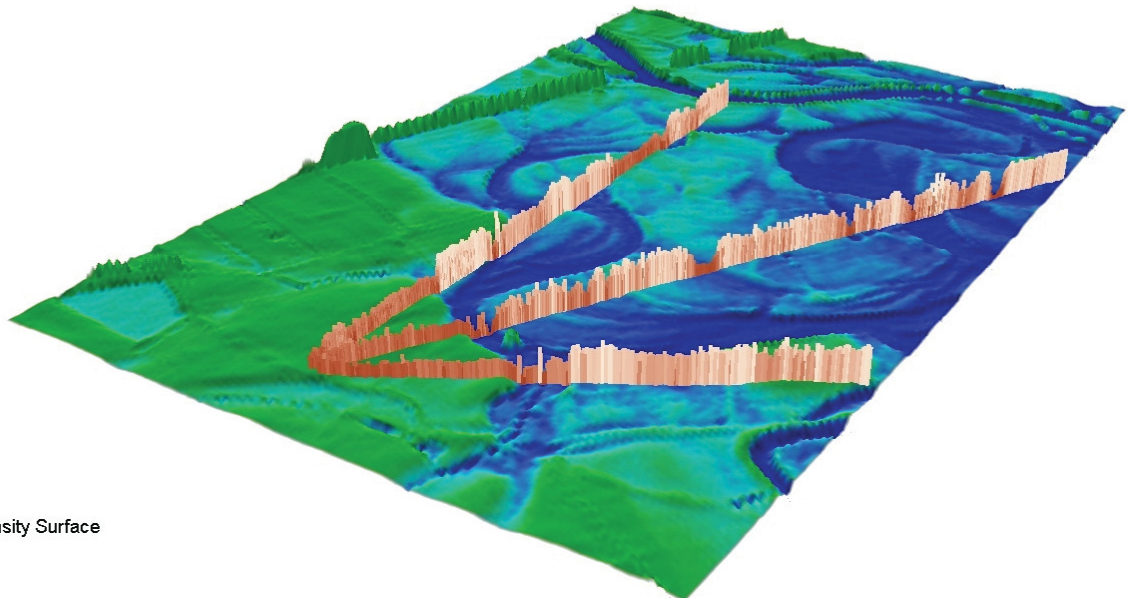
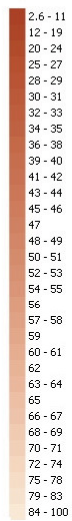
² Institute of Antiquity and Archaeology, University of Birmingham

³ Birmingham Archaeology & HP Visual & Spatial Technology Centre

⁴ University of Leicester Archaeological Services (ULAS),

June 2005

LiDAR Intensity Profiles



LiDAR Intensity Surface



I. Executive Summary

This report describes a multi-method to characterise the archaeological resource of a complex confluence zone between two rivers in the East Midlands, UK (Trent and Soar). The aims of the project centred upon the evaluation of LiDAR, IFSAR and GPR for the semi-automated production of a chronostratigraphic model that could be related to traditional techniques of data collection such as geomorphological survey and plotting of the archaeological resource. The results showed that LiDAR last pulse return produced an accurate DTM, which defines the topographical complexity of the area. The results were found to be very comparable to geomorphological mapping. IFSAR data was found to reveal less of the subtle within terrace/unit variation identified by LiDAR but still identified the terrace sequence.

GPR transects provided technical experience in the survey of such complex alluvial terrain. GPR survey performed well on the gravel bodies including the terraces and agreed well with gouge auger surveys. GPR could resolve the edge of terraces and palaeochannels but not the internal stratigraphy or depth of the deeper and lowest palaeochannels due to a combination of radar absorbent silt and clay and a high water table. GPR survey revealed that the LiDAR intensity of return data appeared to reflect the sub-surface stratigraphy probably through variations in soil moisture. Archaeological resource evaluation showed that the pattern of finds was a result of differential erosion and deposition, visibility and intensity of survey. The high archaeological resource of the area is probably due to it being a transport node but this resource is buried in zones of the valley floor of different ages and modes of deposition.

Along with geomorphological mapping LiDAR and GPR were able to resolve the valley floor into three surfaces and a number of individual features. Using a combination of geomorphological mapping, dGPS, IFSAR, LiDAR and GPR a predictive chronostratigraphic model of the confluence zone was produced. This model will be tested in phase II by coring, sediment characterization and a dating programme.

II. Acknowledgements

This report has been written with the considerable support and help from many individuals. Technical and cartographic advice is acknowledged from S. Rouillard, H. Jones and D. Fraser. The landowners of the target area must be thanked for access and in particular Lafarge Aggregates Ltd. for both access and the provision of data.

III Contents

- I. Executive Summary
- II. Acknowledgements
- III. Contents
- IV. List of figures
- V. List of tables

CHAPTER 1: INTRODUCTION

- 1.1 SUMMARY OF AIMS AND OBJECTIVES
- 1.2 THE STUDY AREA
- 1.3 PROJECT BACKGROUND
- 1.4 PREVIOUS WORK

CHAPTER 2: PROJECT AIMS AND OBJECTIVES

CHAPTER 3: MATERIALS AND METHODS

- 3.1 LiDAR
- 3.2 IFSAR
- 3.3 Aerial photography
- 3.4 Materials and methods Ground Penetrating Radar
 - 3.4.1 *The Ground Penetrating Radar (GPR) and application in alluvial environments*
 - 3.4.2 *GPR survey aims*
 - 3.4.3 *GPR transect and grid plan data capture*
 - 3.4.4 *Choice of survey areas*
 - 3.4.5 *Transect spacing*
 - 3.4.6 *Grid sizes*
 - 3.4.7 *GPR survey in alluvial environments*
 - 3.4.8 *GPR configuration*
 - 3.4.9 *Field survey*
 - 3.4.10 *GPR processing*

3.5 Transect coring

3.6 Geomorphological mapping

3.7 Data archive and query

3.8 Integration of Remote sensed and ground based prospection methods

CHAPTER 4: RESULTS FROM REMOTE SENSED DATA

4.1 Floodplain and Terrace Geomorphology

4.2 Cultural Archaeology

4.3 Flooding on the River Trent

4.4 LiDAR Digital Surface Models

4.4.1 LiDAR Digital Surface Models and Geoarchaeological Mapping

4.4.2 LiDAR DSM results

4.5 LiDAR DSM Spatial Resolution

4.5.1 Absolute Accuracy of the LiDAR DSM

4.5.2 Relative Accuracy and Resolving Ability of the LiDAR DSM

4.6 Resolving Ability of the Resampled DSM

4.7 LiDAR Laser Intensity

4.8 Laser Intensity and Cropmark Formation

4.8.1 LiDAR Intensity and Cropmark Formation

4.9 LiDAR Intensity and Topography

4.10 Soil Moisture and Laser Intensity

4.11 Inteferometric Synthetic Aperture Radar

4.11.1 IFSAR DSM

4.11.2 IFSAR ORI

CHAPTER 5: THE GROUND PENETRATING RADAR SURVEYS

5.1 The GPR surveys on the modern floodplain

5.1.1 Modern floodplain transect 1

5.1.2 Modern floodplain grid 1 survey (MFG1)

5.1.3 Modern floodplain grid 2 high resolution survey (MFG2)

5.1.4 Summary of the GPR results from the modern floodplain

5.2 The GPR surveys on terrace 1

5.2.1 Terrace 1 transect 1 (T1T1)

5.2.2 Terrace 1 quarry transect T1QT

5.2.3 Terrace 1 grid 1 and terrace 1 transect 2 (T1G1 and T1T2)

5.2.4 Terrace 1 Grid 2 survey (T1G2)

5.2.5 T1 G3 survey

5.2.6 Summary of the GPR surveys on the middle unit

5.3 The GPR surveys on terrace 2

5.3.1 Terrace 2 transect 1 (T2T1)

5.3.2 Terrace 2 grid 1 survey (T2G1)

5.3.3 Summary of the GPR surveys on the upper unit

5.4 Comparison of the GPR surveys with bore hole data

CHAPTER 6: DATA INTEGRATION OF REMOTE SENSED AND GROUND PENETRATING RADAR SURVEY DATA

6.1 Integration in ArcScene

6.1.1 Integration of MFG1 and LiDAR data

6.1.2 Integration of T1G1 and LiDAR

6.1.3 Integration of T1G3 and LiDAR

6.1.4 Integration of T2G1 and LiDAR

CHAPTER 7: GEOLOGY AND GEOMORPHOLOGICAL MAPPING

7.1 Geology

7.2 Geomorphological Mapping

CHAPTER 8: ARCHAEOLOGICAL ASSESSMENT OF THE STUDY AREA AND ITS ENVIRONS

8.1 Lower-Middle Palaeolithic

8.2 Upper Palaeolithic

8.3 Mesolithic

8.4 Neolithic – Mid Bronze Age

8.5 Late Bronze Age – Iron Age

8.6 Romano-British

8.7 Anglo-Saxon

8.8 Medieval

8.9 Post-medieval

8.10 Geomorphology and the archaeological resource

8.11 Conclusions

CHAPTER 9 : CRONOSTRATIGRAPHIC MODELLING

9.1 Methodology

9.2 The Chronostratigraphic Cross-section

CHAPTER 10: CONCLUSIONS AND FUTURE DIRECTIONS

IV LIST OF FIGURES AND TABLES

Chapter 1

Fig 1.1: The study area over the 1:50,000 Ordnance Survey map (by permission of OS).

Chapter 3

Fig 3.1: The GPR survey areas within the overall study area.

Fig 3.2: The GPR survey about to start on the modern floodplain, using a 200MHz antenna.

Chapter 4

Fig 4.1: Map showing the drift geology of the study area.

Fig 4.2: Geocorrected vertical air-photographs of the northeast corner of the study area taken on 2nd December 1946.

Fig 4.3: Geocorrected vertical aerial photograph mosaic of the study area taken on 15th December 1954.

Fig 4.4: Geocorrected vertical aerial photograph of the study area taken on 28th June 1976.

Fig 4.5: Map summarising the fluvial geomorphological features across the study area.

Fig 4.6: Map summarising cultural archaeological remains transcribed from air-photographs.

Fig 4.7: December 1954 vertical aerial photograph of the study area taken when the Rivers Trent and Soar were in flood.

Fig 4.8: Pseudo 3D view of a LiDAR derived simulation of the extent of flooding of the study area on 15th December 1954.

Fig 4.9: The December 1954 aerial photograph of the study area with LiDAR laser intensity data superimposed.

Fig 4.10: Two views of point cloud LiDAR elevation data for a part of the study area.

Fig 4.11: LiDAR first pulse digital surface model of the study area.

Fig 4.12: LiDAR last pulse ground digital surface model of the study area.

Fig 4.13: Last Pulse Ground (Left) and First Pulse (Right) LiDAR DSM of the study area with below, profiles through the two DSM illustrating the facility of the LPG DSM to show the ground surface of palaeochannels beneath vegetation cover.

Fig 4.14: LiDAR laser intensity data for the study area.

Fig 4.15: Comparison of (A) LiDAR laser intensity (B) LiDAR DSM and (C) air-photographic evidence for palaeochannels within the floodplain and Hemington Terrace.

Fig 4.16: Comparison of (A) LiDAR laser intensity (B) LiDAR DSM and (C) air-photographic evidence for palaeochannels within the Hemington Terrace.

Fig 4.17: LiDAR laser intensity data for the study area with red lines indicating the location and extent of the 12 study transects.

Fig 4.18: Profiles 1 and 2 showing from top to bottom, RTK GPS elevation values, LiDAR LP DSM, LiDAR Intensity, IFSAR DSM, simulated 2m, 5m and 10m LiDAR DSM.

Fig 4.19: Profiles 3 and 4 showing from top to bottom, RTK GPS elevation values, LiDAR LP DSM, LiDAR Intensity, IFSAR DSM, simulated 2m, 5m and 10m LiDAR DSM.

Fig. 4.20: Profiles 5 and 6 showing from top to bottom, RTK GPS elevation values, LiDAR LP DSM, LiDAR Intensity, IFSAR DSM, simulated 2m, 5m and 10m LiDAR DSM.

Fig 4.21: Profiles 7 and 8 showing from top to bottom LiDAR LP DSM, LiDAR intensity and IFSAR DSM.

Fig 4.22: Profiles 9 and 10 showing from top to bottom LiDAR LP DSM, LiDAR intensity and IFSAR DSM.

Fig 4.23: Profiles 11 and 12 showing from top to bottom LiDAR LP DSM, LiDAR intensity and IFSAR DSM.

Fig 4.24: Simulated 2m LiDAR Last pulse ground digital surface model.

Fig 4.25: Simulated 5m LiDAR Last pulse ground digital surface model.

Fig 4.26: Simulated 10m LiDAR Last pulse ground digital surface model.

Fig 4.27: LiDAR DSM of an area of earthwork ridge and furrow in the southeast corner of the study area showing the impact of variations in spatial resolution.

Fig 4.28: LiDAR DSM of the earthworks of the Bull Ring in the northwest corner of the study area showing the impact of variations in spatial resolution.

Fig 4.29: Elevation (left) and slope (right) histograms for LiDAR 1mFP, 1mLP and 2m DSM data for the entire study area.

Fig 4.30: Elevation (left) and slope (right) histograms for LiDAR 5m, and 10m DSM data for the entire study area.

Fig 4.31: Pseudo 3D view of the LiDAR LP DSM of the study area colour shaded to reflect variations in laser intensity.

Fig 4.32: Comparison of (A) cropmark evidence on air-photography, (B) LiDAR intensity, (C) intensity and cropmark evidence merged and (D) cropmark plot, for the later prehistoric settlement complex AND Romano-British villa at Lockington.

Fig 4.33: Comparison of (A) cropmark evidence on air-photography, (B) LiDAR intensity, (C) intensity and cropmark evident merged and (D) cropmark plot, for the Lockington villa.

Fig 4.34: Comparison of (A) cropmark evidence on air-photography, (B) LiDAR intensity, (C) intensity and cropmark evident merged and (D) cropmark plot, for the later prehistoric settlement complex at Lockington.

Fig 4.35: Comparison of (A) cropmark evidence on air-photography, (B) LiDAR intensity, (C) intensity and cropmark evident merged and (D) cropmark plot, for the small sub-square enclosure at SK484300.

Fig 4.36: Comparison of (A) cropmark evidence on air-photography, (B) LiDAR intensity, (C) intensity and cropmark evident merged and (D) geophysical survey plot, for the later prehistoric settlement complex at Warren Lane.

Fig 4.37: LiDAR intensity data for the study area with the locations of *in-situ* volumetric soil moisture readings shown in red.

Fig 4.38: Scatter plots with fitted trend lines showing the relationship between topsoil moisture and LiDAR intensity in each geomorphological zone.

Fig 4.39: Line graph showing standardised variations in volumetric soil moisture in the topsoil (green), subsoil (blue) and LiDAR laser intensity (orange) at each sample location, vertical bars indicate the boundaries between geomorphological units, annotations indicate geomorphological features.

Fig 4.40: Maps showing LiDAR intensity with superimposed bar charts showing volumetric soil moisture readings at the surface (green) at subsoil level (yellow) and corresponding LiDAR intensity value at sample locations 1-4.

Fig 4.41: IFSAR (Radar) 10m digital surface model of the study area.

Fig 4.42: Profiles through the LiDAR and IFSAR DSM of the study area showing the elevation of the major geomorphological units.

Fig 4.43: Left elevation and right slope for IFSAR DSM data for the entire study area.

Fig 4.44: Difference between elevation values recorded by the IFSAR (Radar) 10m digital surface model of the study area and the LiDAR first pulse surface model.

Fig 4.45: IFSAR (Radar) Orthorectified Radar Image (ORI) of the study area.

Fig 4.46: IFSAR ORI of selected parts of the study area.

Chapter 5

Fig 5.1: The location of the MFT1 transect on the modern floodplain.

Fig 5.2: The MFT1 transect, shown with the gouge core transect and also with an interpretation of the data.

Fig 5.3: The LiDAR intensity plot over the MFG1 survey area, highlighting palaeochannels MFC1, MFC2 and MFC3.

Fig 5.4: The LiDAR last pulse DTM showing the surface topographic features within the MFG1 survey area.

Fig 5.5: The T1G1 survey 0.85m – 1.15m depth slice. The gravel units MF3 and MF4 are clearly visible, as are the palaeochannels MFC2 and MFC3.

Fig 5.6: The MFG1 survey, 0.35m – 1.45m depth slice. MF3 is again the dominant feature, with the palaeochannels MFC2 and MFC3 evident.

Fig 5.7: The MFG1 survey, at the 1.85m – 2.15m depth slice.

Fig 5.8: A comparison of the effect of different transect intervals on data quality using the MFG1 survey 0.85m – 1.15m depth slice.

Fig 5.9: A comparison of the effect of different transect intervals on data quality using the MFG1 survey 1.35m – 1.65m depth slice.

Fig 5.10: The location of the MFG2 survey, shown on the LiDAR last pulse DTM.

Fig 5.11: The MFG2 survey 0.2m – 0.3m depth slice.

Fig 5.9: A comparison of the effect of different transect intervals on data quality using the MFG1 survey 1.35m – 1.65m depth slice.

Fig 5.12: The MFG2 survey, 0.45m – 0.55m depth slice. The features of MF3, MFC1, MF7 and MF8 visible.

Fig 5.13: The MFG2 survey at the 0.7m – 0.8m depth slice.

Fig 5.14: The location of the T1T1 survey on terrace 1.

Fig 5.15: The T1T1 transect, shown with interpretation and corresponding gouge core data.

Fig 5.16: A rectified aerial photograph showing the T1T1 survey area.

Fig 5.17: The location of the T1QT survey.

Fig 5.18: The T1QT survey, shown with interpretation and against the section drawing.

Fig 5.19: A photograph of the start of the T1QT transect, showing the main units from the GPR interpretation.

Fig 5.20: Within the gravel unit on terrace 1 were substantial organic remains, such as these three oak trees.

Fig 5.21: The LiDAR last pulse DTM, showing terrace 1 and the palaeochannel T1C6. The location of T1T1 is also shown.

Fig 5.22: The LiDAR intensity plot, also showing a difference between terrace 1 and T1C6.

Fig 5.23: A flood simulation, through combining an aerial photograph of the 1954 flood with the LiDAR last pulse DTM.

Fig 5.24: The T1T2 transect survey, shown with an interpretation and against gouge core data.

Fig 5.25: The T1G1 survey, 0.9m – 1.1m depth slice.

Fig 5.26: The T1G1 survey, 1.4m – 1.6m depth slice.

Fig 5.27: The T1G1 survey, 1.9m – 2.1m depth slice, with the gravel unit T1H2 clearly visible.

Fig 5.28: The T1G1 survey, 2.4m – 2.6m depth slice.

Fig 5.29: The LiDAR last pulse DTM of the T1G2 survey area.

Fig 5.30: The LiDAR intensity over the T1G2 survey area.

Fig 5.31: The T1G2 survey, 0.4m – 0.6m depth slice.

Fig 5.32: The T1G2 survey, at the 0.9m – 1.1m depth slice.

Fig 5.33: The T1G2 survey, 1.4m – 1.6m depth slice.

Fig 5.34: The T1G2 survey, 1.9m – 2.1m depth slice.

Fig 5.35: The T1G2 survey, 2.4m – 2.6m depth slice.

Fig 5.36: The T1G2 survey, 2.9m – 3.1m depth slice.

Fig 5.37: A pseudo 3D section produced through Radan, showing the relationships of T1H4, T1H3 and T1C7.

Fig 5.38: The LiDAR last pulse DTM over the T1G3 survey area.

Fig 5.39: The LiDAR intensity plot over the T1G3 survey area.

Fig 5.40: The T1G3 survey, 0.4m – 0.6m depth slice.

Fig 5.41: The T1G3 survey 0.9m – 1.1m depth slice.

Fig 5.42: The T1G3 survey, 1.4m – 1.6m depth slice.

Fig 5.43: The location of the T2T1 transect, shown on the LiDAR last pulse DTM.

Fig 5.44: A rectified aerial photograph of the T2T1 survey area, showing a possible palaeochannel, T2C1.

Fig 5.45: The T2T1 GPR transect shown with interpretation and against the gouge core transect.

Fig 5.46: LiDAR last pulse DTM over the T2G1 survey area.

Fig 5.47: The LiDAR intensity values across the T2G1 survey area.

Fig 5.48: The T2G1 survey, 0.4m – 0.6m depth slice.

Fig 5.49: The T2G1 survey, 0.9m to 1.1m depth slice.

Fig 5.50: The T2G1 survey, 1.4m – 1.6m depth slice.

Fig 5.51: The T2G1 survey, 1.9m – 2.1m depth slice.

Fig 5.52: The T2G1 survey, 2.4m – 2.6m depth slice.

Fig 5.53: The T2G1 survey, 2.9m – 3.1m depth slice.

Fig 5.54: The location of five bore holes within the survey area.

Fig 5.55: The stratigraphy of the boreholes.

Chapter 6

Fig 6.1: The LiDAR last pulse DTM combined with the 1.4m – 1.6m and 2.4m – 2.6m depth slices on the MFG1 survey.

Fig 6.2: The T1G1 survey combining the GPR depth slices of 0.4m – 0.6m, 0.9m – 1.1m, 1.9m – 2.1m and 2.4m – 2.6m with the LiDAR intensity.

Fig 6.3: The T1G3 survey combining the GPR depth slices of 0.4m – 0.6m, 1.4m – 1.6m and 2.4m – 2.6m with the LiDAR last pulse DTM.

Fig 6.4: The T2G1 survey combining the GPR depth slices of 0.4m – 0.6m, 1.4m – 1.6m and 2.4m – 2.6m with the LiDAR intensity.

Chapter 7

Fig 7.1: The lithology map of the study area.

Fig 7.2: The drift geology of the study area.

Fig 7.3: The geological stage map of the study reach.

Fig 7.4: Geomorphological map of the study reach.

Fig 7.5: Profile 1 generated from the LiDAR DTM.

Fig 7.6: Profile 2 generated from the LiDAR DTM.

Fig 7.7: Profile 3 generated from the LiDAR DTM.

Chapter 8

Fig 8.1: The study area mapped by geological stage.

Fig 8.2: The archaeological resource plotted by its method of investigation.

Fig 8.3: The archaeological resource plotted by period.

Fig 8.4: The ‘Lockington Villa’ complex within the study area.

Fig 8.5: The cropmark enclosure on terrace 1.

Chapter 9

Fig 9.1: Chronostratigraphic model map of the Trent-Soar Junction.

Fig 9.2: Hypothesised cross section across the study area.

V. LIST OF TABLES

Chapter 3

Tab 3.1: The GPR surveys.

Chapter 4

Tab 4.1: Summary of vertical sorties containing good evidence of fluvial geomorphology within the study area.

Tab 4.2: Statistics for the various LiDAR DSM and derived slope values.

Tab 4.3: Tabulated coefficients of correlation between volumetric moisture of topsoil, subsoil and LiDAR Intensity for each geomorphological zone.

Tab 4.4: Tabulated volumetric soil moisture and corresponding LiDAR intensity data also showing standardised values.

Tab 4.5: Statistics for the IFSAR DSM and derived slope values.

Chapter 9

Tab 9.1: Data sources used in the chronostratigraphic modelling.

CHAPTER 1: INTRODUCTION

This project was framed to address the core ALSF theme of developing capacity to manage aggregate extraction landscapes in the future (English Heritage 2004). In addition it addresses several other ALSF themes, namely:

- Characterising the (archaeological) resource and developing evaluation frameworks, predictive tools and mitigation strategies.
- Development [of] remote sensing and predictive techniques and mitigation strategies.
- Training and professional development: to raise awareness of issues and to improve the quality of historic environment work undertaken in response to aggregate extraction.
- Development of advanced visualisation and immersive three-dimensional models of landscape development. Although largely part of phase 2 of the project, this has the potential to address the theme of interpretation and outreach to the community of the knowledge gained from work related to aggregate extraction.

1.1 Summary of aims and objectives

The aim of this project is to predictively model the landscape of a major river confluence over a time-scale of millennia and at a spatial scale appropriate for archaeological management. The overall purpose is:

- To establish a RIGOROUS research model for the future development of predetermination designs for site evaluation.
- To assess the effectiveness of various airborne and ground based remote sensing methods in alluvial environments.
- To derive relationships between pre-extraction site survey data and likely chronostratigraphic and environmental data as part of archaeological assessment.

This research will assist regulatory bodies (i.e. County Councils) in demanding and specifying rapid evaluations of geoarchaeological potential as part of the implementation of PPG16. The novelty of the approach lies in the integration of high-resolution topographical, archaeological and geological (three-dimensional sub-surface) data within a Geographical Information System (GIS). The technical innovation will be the combination of Interferometric Synthetic Aperture Radar (IFSAR), Airborne Laser Altimetry (LiDAR), CW Differential GPS (DGPS), Ground Penetrating Radar (GPR) and other ground based remote sensing techniques. This research will contribute to the framework for management of the archaeological resource in the Trent Valley developed through Trent Valley GeoArchaeology (Bishop *et al.* 2002) and provide a transferable model for the geoarchaeological investigation and management of valley floor archaeology.

1.2 The study area

The study area is a block of the Trent/Soar confluence landscape approximately 2 by 4 km (Fig. 1.1). The area abuts the main area of Trent Valley GeoArchaeology (TVG) interest and is close to but not overlapping sites of continuing research by University of Leicester Archaeological Services (ULAS). The area is not zoned for aggregate extraction although the area to the west is. Extraction of these adjacent areas will allow boundary sedimentary information to be used in modelling.

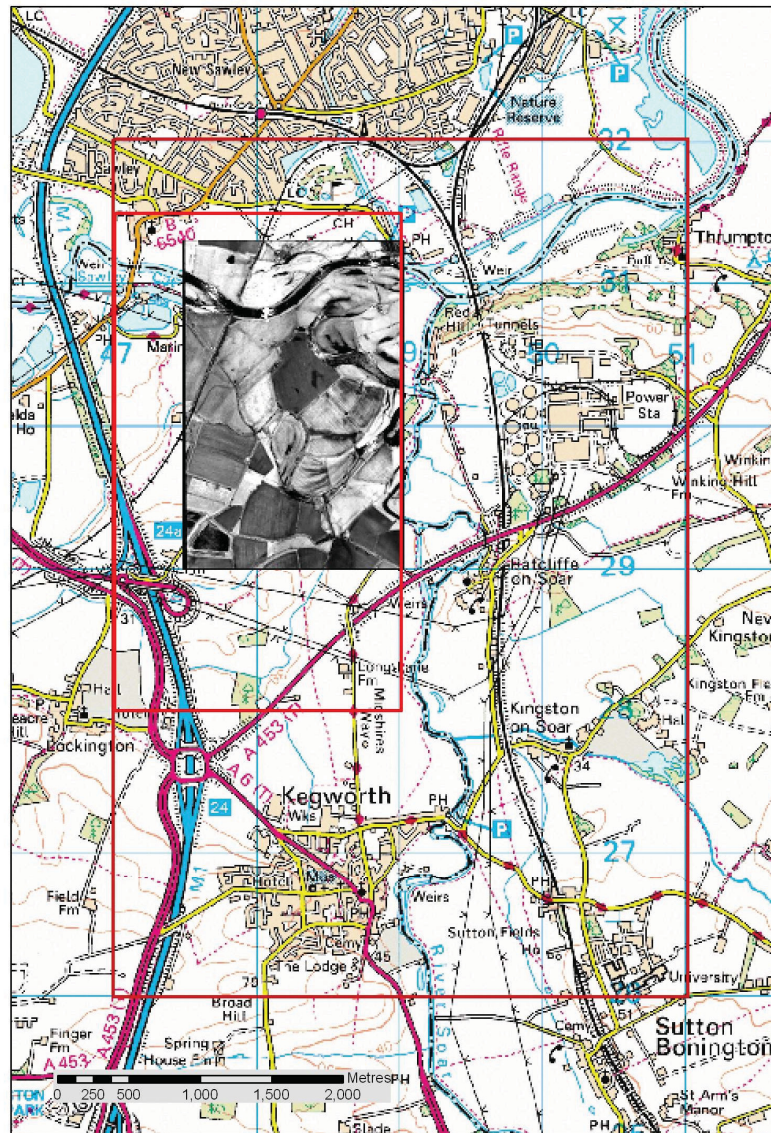


Fig 1.1: The study area over the 1:50,000 Ordnance Survey map (by permission of OS).

1.3 Project background

Recent archaeological work on the Thames and other British floodplains suggests that river confluences have been the foci of settlement and human activity since the earliest post-glacial periods. At confluences the high density of palaeochannels provides an opportunity to determine records of past environmental change. Migration of rivers channels also provides an environment with high potential for the burial and preservation *in situ* of cultural and environmental materials. Unfortunately this potential is generally only realised during the destruction of the land surface by development and subsequent 'rescue' archaeological investigation.

It is the nature of the archaeological record of floodplains that there is a direct link between the geomorphology, including the nature and distribution of channels, levees, gravel bars, terrace remnants, etc. and the distribution and nature of archaeological materials, from flint scatters to structures. Therefore there is a predictive capability in the subsurface geomorphology, stratigraphy and buried land surfaces.

1.4 Previous work

The Middle Trent is one of the archaeologically richest stretches of alluvial landscape in the UK. Finds include medieval bridges (the Hemington Bridges excavations, funded by English Heritage), a Norman milldam, fishweirs and dugout canoes (Salisbury *et al.*, 1984; Cooper, 2003). The study area (a block of floodplain 8 km²) is centred on the Lockington Marshes at the confluence of the Trent and Soar. This area is rich in cultural archaeology lying immediately east of the nationally significant prehistoric ritual landscape of the Derbyshire Trent Valley (Riley, 1987). Recent finds from a Bronze Age barrow cemetery (Hughes, 2000) strongly suggests that this prehistoric ritual landscape extends into the area. In the Romano-British period the area lies in the hinterland of a villa complex at Lockington and a small town, possibly a centre of ritual/religion at Red Hill, Ratcliffe on Soar (Elsdon, 1982). The area, although not threatened with imminent destruction, is earmarked for longer-term development. Pilot studies indicate the high buried archaeological potential of the locality (Ripper, 1997), which combined with a high density of sites suitable for palaeoenvironmental studies (Howard, 1997) provide an ideal zone for detailed modelling. Work by Trent Valley GeoArchaeology (Knight and Howard, 2004) has done much to provide a regional framework for the cultural, landscape and environmental archaeology of the Trent Valley. The present proposal provides an opportunity to build constructively on that framework through detailed consideration of a significant confluence zone, targeted fieldwork and innovative use of GIS and allied technologies.